Dynamic characterization of machining systems

Miron Zapciu, Jean-Yves K'Nevez, Alain Gérard, Olivier Cahuc, Claudiu-Florinel Bisu

International Journal of Advanced Manufacturing Technology manuscript No.
(will be inserted by the editor)

M. ZAPCIU · J-Y. K'nevez · A. Gérard · O. Cahuc · C. F. Bisu

Dynamic characterization of machining systems.

Received: 28 October 2010 / Accepted: 13 Febrary 2011

Abstract In the working space model of machining, an experimental procedure is implemented to determine the elastic behaviour of the machining system. In this paper, a dynamic characterization and vibration analysis has long been used for the detection and identification of the machine tool condition. The natural frequencies of the lathe machining system are required (Ernault HN400 - France) according to three different situations with no cutting process are acquired. The system modal analysis is used to identify the natural frequencies. These frequencies are then compared to the ones obtained on the spindle numerical model by Finite Element Method. This work is validated by experimental tests based on measures of the lathe machine tool frequencies domain. The main objective is to identify a procedure giving the natural frequencies values for the machine tool components, in order to establish a better condition in the cutting process of the machine tool.

Keywords: Dynamic characterization; Machining system; Natural frequencies analysis.

A. Gérard (corresponding author) · J-Y. K'nevez · O. Cahuc
Université de Bordeaux et CNRS UMR 5295,
351 cours de la Libération, 33405 Talence-cedex France (UE)
Tel.: +33 (0)5 40 00 62 23
Fax: +33 (0)5 40 00 69 64
E-mail: alain.gerard@u-bordeaux1.fr

M. Zapciu · C. F. Bisu
University Politehnica from Bucharest,
313 Splaiul Independentei, 060042 Bucharest Roumanie (UE)

Nomenclature

BT	Block Tool
BW	Block Workpiece
$[C]$	Damping matrix
D_1	Holding fixture diameter (mm)
D_2	Workpiece diameter (mm)
$f_{sampling}$	Sampling frequency (Hz)
f_{max}	Highest frequency component in the measured signal (Hz)
$[K]$	Stiffness matrix (N/m)
L_1	Holding fixture length (mm)
L_2	Workpiece length (mm)
$[M]$	Mass matrix (kg)
T	Period (s)
x (z)	Cross (feed) direction
y	Cutting axis
WTM	Workpiece-Tool-Machine
ω_d	Damped natural frequency
ξ	Percentage of damping

1 Introduction

Metal cutting is one of the most important manufacturing processes. The most common cutting processes are milling, drilling, grinding and turning. These processes help outline the parts and also as soon as requirements of the dimensional tolerance, precision or the quality of the surfaces of the produced part appear. However, these dimensional accuracies and the final shape of the part (controlled roughness) often depend on the vibrations appearance during the process [36].

In the cutting process, the vibration is a dynamically unstable phenomenon [41]. These instabilities, often regenerative, are generated by many factors such as the workpiece flexibility and tools properties materials, the machine rigidity, tool geometry (approaching angle, rake angle, etc.) and the cutting tool edge radius, the nominal cutting conditions such as tool wear, feed rate and depth of cut, [13] etc. Thus, the knowledge of

the machining system elastic behaviour is essential to understand the cutting process [8].

For many reasons, the cutting process' stability is very intensely studied particularly its the influence on the final surface quality [12], [39], [14]. The ordering of the process under various work conditions is an important problem for machining. A large amount of modeling in implemented in order to optimize the cutting conditions, [19], [4], [20], [40]. The orthogonal cut is the process that drives the attention more because of its simplicity in implementation [18].The regenerative aspect induced by the surface previously machined which has a sinusoidal form (waviness on the surface) is an example. Taking into account the nonlinear interaction between the tool and its part almost always gives interesting results which go from regular (periodic or quasi-periodic) vibrations to possibilities of chaotic ones [26] or, always within the orthogonal framework of the cut, while utilizing in more the dry friction [27].

The 2D case is also examined while considering its rigid part but by also taking into account the tool flexibility [9], [17] the tool holder flexibility [12] or the rotor system [33]. Dassanayake et Al. approach the case of the workpiece dynamic response to the tool request which follows a regenerative surface [16], [41]. All the modeling reaches interesting results, but, in general, does not take into account the whole of the kinematic chain of the cutting process. We want to describe the entire kinematic chain of the cutting process thereafter in a digital richer model and brought closer to the experimental data.

The analysis of the machines' dynamic behaviour is an important method to redesign the product or the manufacturing process and to assure the proper quality, maintenance and service [1]. When machines or only parts of them are studied, the dynamic behaviour is analysed in the following situations:

- Constant operating speed (e.g. speed rate of a rotor);
- Variable speed into a limited operating domain;
- Imposed speed inside the operational domain (e.g. rotational speed of the spindle 100 to 60,000 rpm);

In all of these mentioned cases the system behaviour under the external excitation effect is evaluated (figure 1).

The transfer function is evaluated as being the ratio response of the system / dynamic excitation. To diagnose one machine or equipment the main characteristics offered by the transfer function are:

- Dynamic rigidity or compliance;
- Resonance frequencies;
- Damping factor;
- Natural modes of vibration.

By measuring the vibratory severity, we find out if the vibratory behaviour of a machine exceeds the acceptable limits or not [11]. But within results sight, it is not possible to make an assumption on the vibration causes. This information could not be obtained by using a frequency spectrum analysis [38].

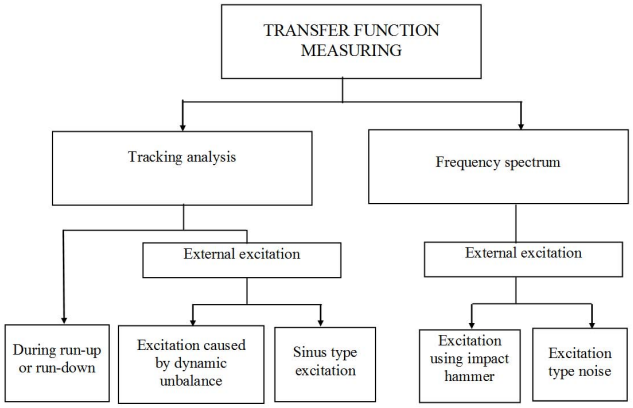

Fig. 1 Transfer function.

We want to establish a model of three-dimensional turning processes as close as possible to the physical reality. Thus, this paper aims at testing a methodology which allows us to characterize the band width of frequencies associated with the unit of each element of the kinematics chain apart from any operation of machining. Also, the tasks to perform the frequency analysis are described in figure 2. In section 2 we present the experimental device with the plan of frequency spectrum acquisition and the experimental results. A finite element analysis is used in order to find the first twelve natural frequencies. Those natural frequencies confirm the first natural frequencies of the system spindle and the system spindle with workpiece. An example of experimental results illustrating a consequence of the vibrations of the machine tool is given in the Section 3. Before concluding, the machine tool dynamic characterization is the detailed in Section 4.

2 Experimental vibration analysis

2.1 *Experimental device*

All machines vibrate and, as the state of the machines worsens (imbalance of the spindle or other important shaft, defect of bearing or spindle) the vibration level increases. An ideal indicator on his state, especially dynamic behaviour [19], [9] is obtained while measuring and by supervising the vibration level produced by a machine.

While the increase in machine vibration allows us to detect a defect, the analysis of the machine vibration characteristics allows us to identify its cause. In this way, we can deduce with sufficient precision the time domain, before vibrations become critical.

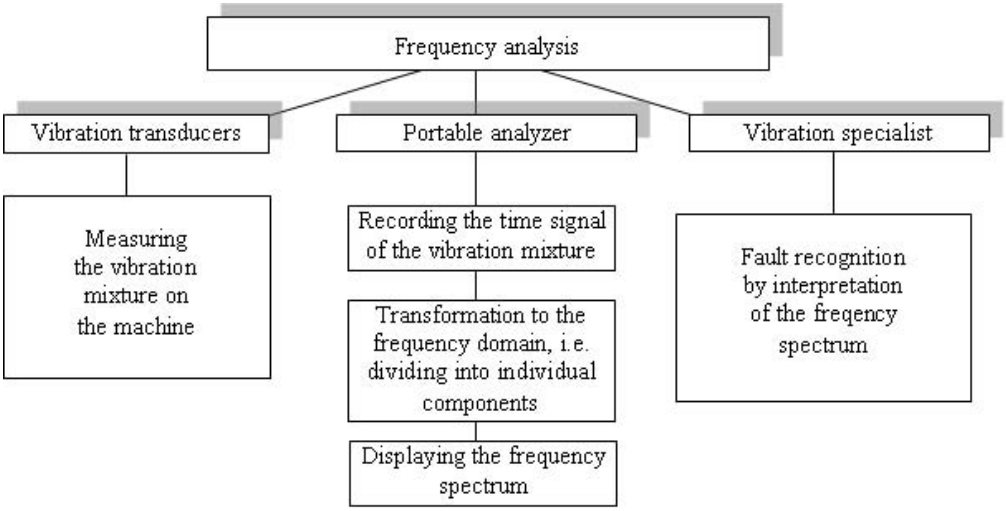

Fig. 2 Frequency analysis tasks for a machine tool.

Each component of spectrum FFT corresponds to a characteristic frequency well defined (imbalance, resonance, misalignment etc.) [24]. The analysis in frequency is generally carried out when the machine vibratory level is considered to be higher than the acceptable threshold [35].

The figure 3 is illustrating the acquisition of the frequency spectrum FFT in the case of the Ernault HN400 lathe - France, LMP Laboratory from University of Bordeaux. Accelerometers were fixed on the horizontal and vertical plans on the bearing fix front part of the lathe spindle.

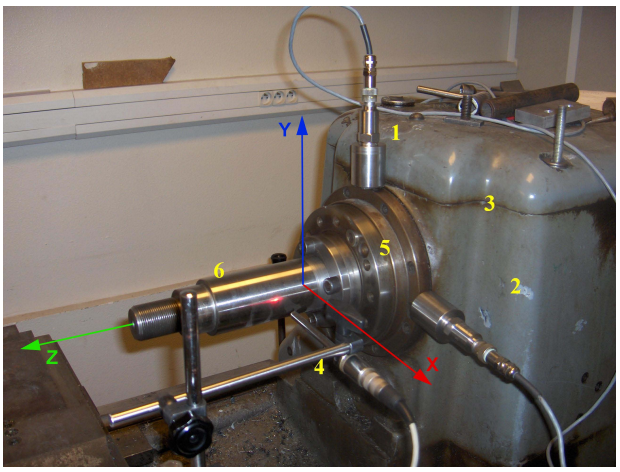

Fig. 3 Position of transducers in acquisition schema to acquire vibrations of the spindle ERNAULT. 1- Accelerometer AS020 -vertical plan (V); 2- Accelerometer AS020 - horizontal plan (H), 3- Gearbox of Ernault HN400 lathe; 4- Tachometer; 5- Spindle bearing front side; 6- Workpiece.

An example of the vibration level of this spindle in horizontal plan is illustrated in the figure 4. Vibration signal versus time was tracked for different spindle speed levels. The vibration speed level in mm/s (rms) is situated in the range 0.1-0.3. For this type of machine tool, in accordance with IEC 34-14 standard the upper limit of the vibration level is 1.8 mm/s (see Table 1).

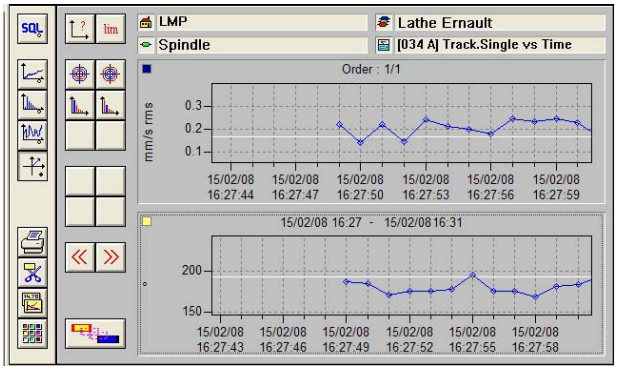

Fig. 4 Vibration level of the Ernault lathe using Tracking versus time procedure.

2.2 *Block Workpiece:* ***BW***

As many authors [4], [43], [30], we chose a cylindrical geometry for the workpiece. The Block Workpiece (**BW**) represents the revolving part of the Workpiece-Tool-Machine system (**WTM**); it includes the holding fixture, the workpiece and the spindle (figure 5). To make the whole frame rigid, a very rigid unit (workpiece, holding fixture) is conceived in front of the **WTM** elements (figure 6).

The workpiece geometry and its holding fixture are selected with $D_1 = 60$ mm, $D_2 = 120$ mm and L_2

Table 1 Limit values in accordance with IEC 34-14.

Related operating speed (rpm)	Limite value of the effective vibration velocity for shaft heights H in mm			
Normal	Machine is mounted on specifically design elastic foundations (e.g. vibration dampers)			Specifically designed rigid foundation
(mm/s)	56 < H < 132	132 < H < 225	H > 225	H > 40
> 600 < 1,800	1.8	1.8	2.8	2.8
> 1,800 < 3,600	1.8	2.8	4.5	2.8

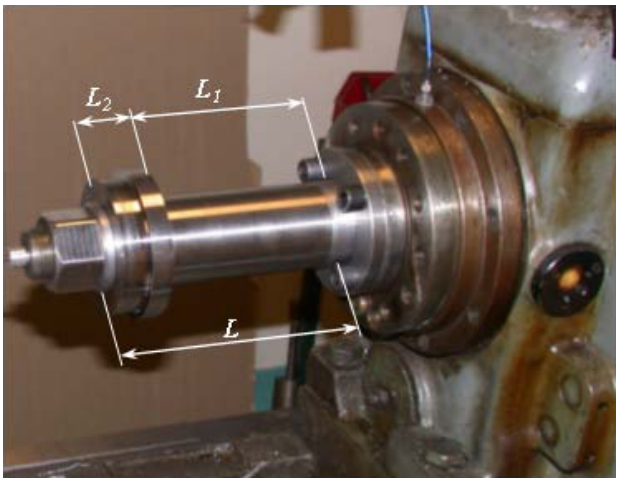

Fig. 5 Representation of the **BW**.

= 30 mm (cf. figure 6).These dimensions retained for these test tubes were selected using the Finite Elements method coupled to an optimization method by SAMCEF® software. It is necessary to determine the holding fixture length L_1 to obtain a significant stiffness in flexion. Usually, the first vibration mode of the Block Workpiece should be at higher frequencies.

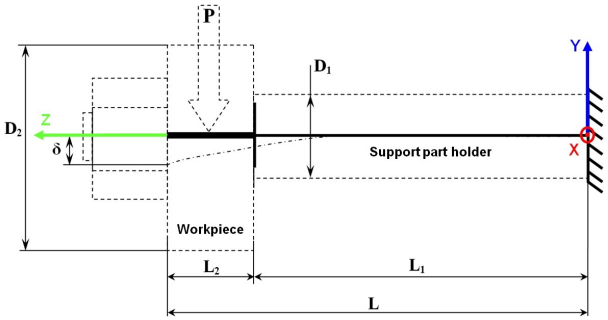

Fig. 6 Geometry of holding fixture / workpiece.

The stiffness is calculated on the basis of the displacement δ for a given force P and a Young modulus $E = 21 \times 10^5$ N/mm^2:

$$\delta = \frac{P.L^3}{3E.I}, \tag{1}$$

with inertial moment :

$$I = \frac{\pi.D_1^4}{64}. \tag{2}$$

A holding fixture length : $L_1 = 180$ mm, for a stiffness in flexion of 7×10^7 N/m, is reminded. This value is in the higher limit of the acceptable zone of rigidity for conventional lathe (cf. figure 7), [32], [21], [22].

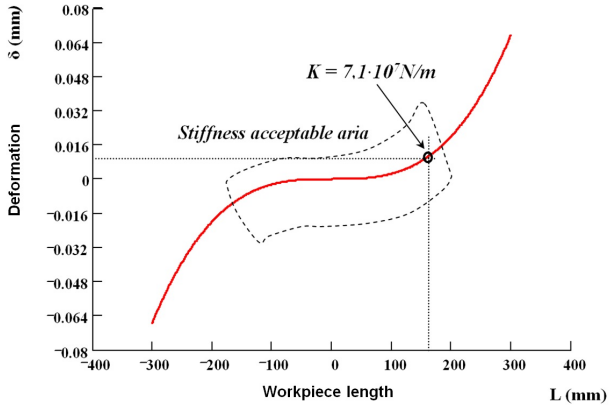

Fig. 7 Representation of the acceptable aria of the workpiece deformation.

2.3 *Block Tool:* ***BT***

In this case, the **BT** part includes the tool, the tool-holder, the dynamometer, the fixing plate on the cross slide (figure 8). The six-components dynamometer [15] is fixed between the cross slide and the tool-holder. It is necessary thereafter for the measurement of the mechanical actions of cutting.

2.4 *Experimental results*

The natural frequencies experimental values obtained following the impact tests are detailed in the figure 9 and 10, considering blocks **BT** and **BW** respectively. Using an impact hammer, the natural frequencies of each block, for each element, are given accordingly the machine axes directions x (cross direction), y (cutting

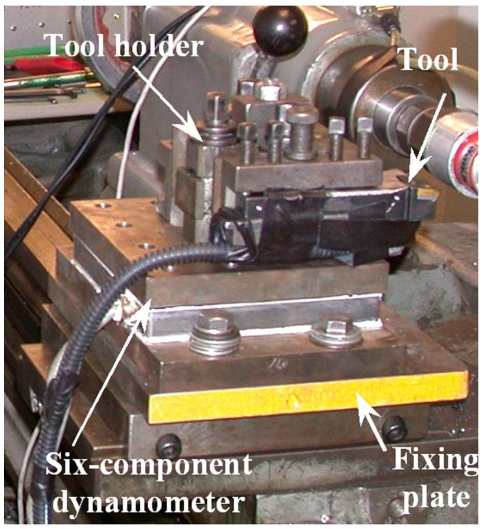

Fig. 8 Representation of the block tool **BT**.

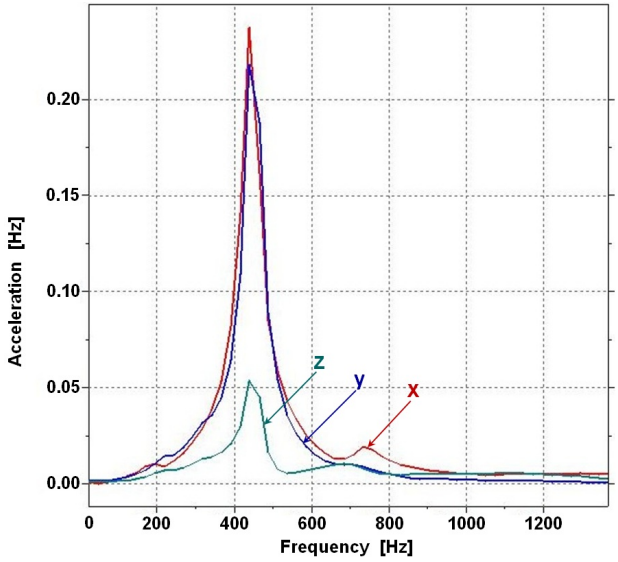

Fig. 10 Natural frequencies for the block-work-piece **BW** (direction: x color red, y color blue, z color green).

direction), and z (feed direction) see figure 3. A three directions accelerometer is positioned on each element, in each direction and the elements tested were the subject of the hammer impact. An example of result is given into the figure 9, where the natural frequencies of whole block **BT** are presented, with all the components.

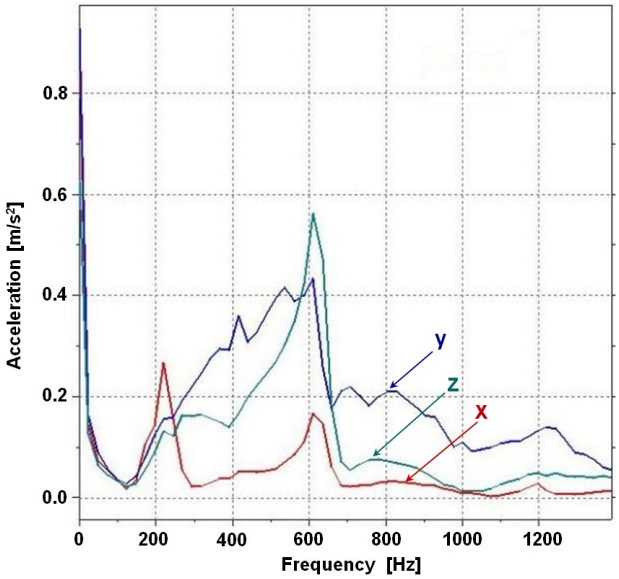

Fig. 9 Natural frequencies representation for the block-tool **BT** (direction : x color red, y color blue, z color green).

The results corresponding to the **BW** unit are presented in the figure 10. The natural frequencies domain is indicated for each component of the system by carrying out a modal superposition in the figure 11. These results are consistent with those met in the literature [32], [29], [10], [34] [23].

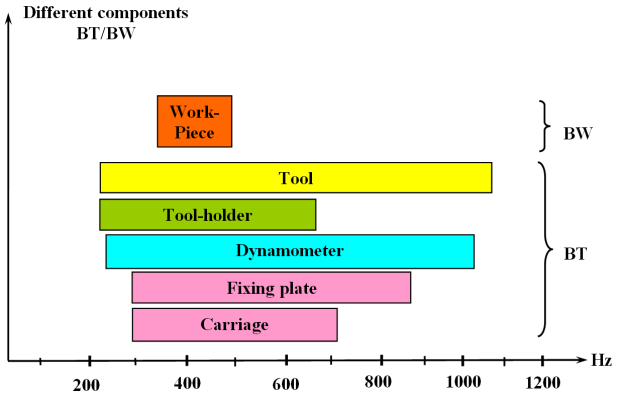

Fig. 11 Natural frequencies domains superposition of the machine tool components at the time of the impact for each element.

Using the layout of the tool free oscillations, (presented in the figure 1), the ξ damping percentage is directly given by the logarithmic decrement curve, starting from N consecutive maximum; the measured period T of the damped oscillations give the damped natural frequency ω_d of the system.

With the obtained values ω_d and ξ, we cannot calculate any damped natural frequency. The values of these parameters allow calculating: the stiffness K, the equivalent mass M and the equivalent damping coefficient C

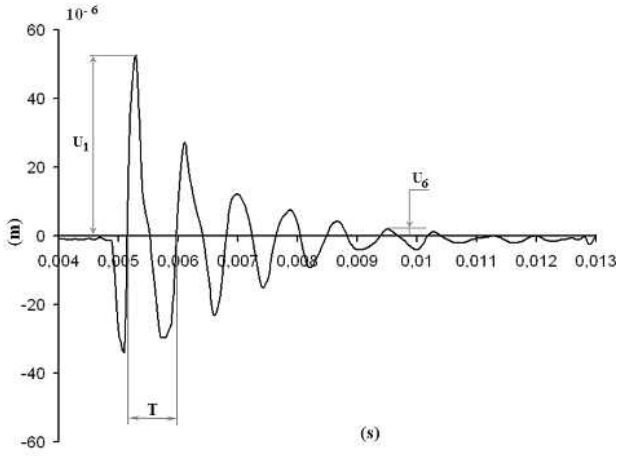

Fig. 12 Test of free displacement during of one impulse using an impact hammer.

for each part **BT** and **BW** and for all three directions. Here is an example for these values.

$$M = \begin{bmatrix} 2.2 & 0 & 0 \\ 0 & 5.3 & 0 \\ 0 & 0 & 2.5 \end{bmatrix}, \tag{3}$$

$$C = \begin{bmatrix} 1.2 \times 10^3 & 0 & 0 \\ 0 & 0.89 \times 10^3 & 0 \\ 0 & 0 & 0.12 \times 10^3 \end{bmatrix}. \tag{4}$$

The stiffness matrix k is given in another work [7].

2.5 *Numerical model of the assembly of the lathe spindle Ernault HN400.*

A finite element analysis was used to find the spindle natural frequencies domain of the machine tool and of the assembly **BW** (spindle with the workpiece attached). The figure 13 shows the mesh (4,290 nodes, 16,310 elements) and spindle numerical model. The figure 14 shows the model by adding the workpiece. In these two cases the boundaries conditions used are: blocked translations and free rotation around z axis (cf. figure 3) .

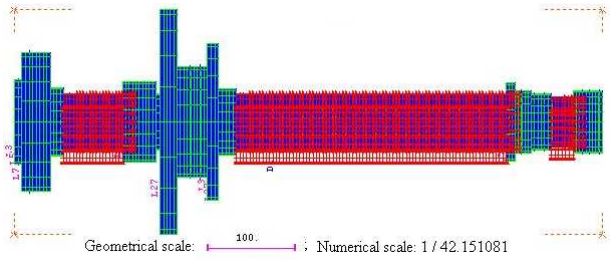

Fig. 13 Spindle numerical model.

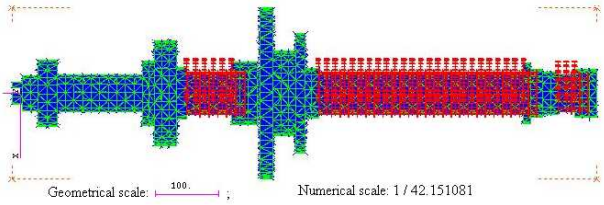

Fig. 14 Spindle with workpiece **BW** numerical model and boundary conditions.

Accordingly numerical models were obtained the results for the first twelve natural frequencies of these two models (represented in the figure 13 and 14). Vibration mode for the first natural frequency is represented in the figure 15 and the numerical values of first twelve natural frequencies are represented in the figure 16.

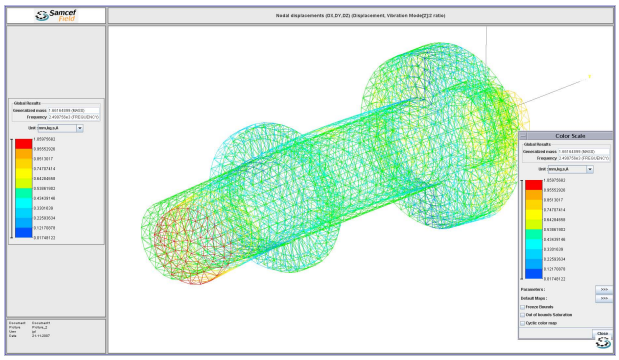

Fig. 15 Vibration bending mode for the first natural frequency.

We can observe that the first spindle natural frequency of the system with workpiece is about 675 Hz and it is lower considering only the spindle system (1,600 Hz). These results are consistent with those experimentally obtained (figure 17).

On the acquired signal FFT spectrum (spindle system turning, without cutting process) we can see the first frequency 675 Hz and, on the right side, the frequency with the value 1,599.1 Hz (corresponding to the spindle alone).

3 Experimental results for chip segmentation frequency in turning

Through the finite element method, Wang et Al. [42] establish that the main reason of the segmented chip formation are the fluctuations of the tool chip contact and the shear band length. However, all contact fluctuations induce vibrations that could induce the segmented chips. The main objective of this section is to check experimentally the relevance of this conjecture in a turning process.

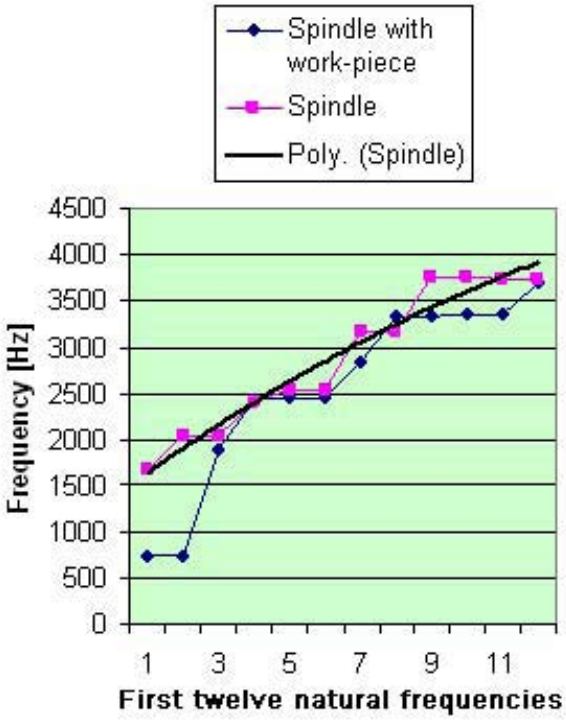

Fig. 16 Spindle natural frequencies polynomial trend of the machine tool.

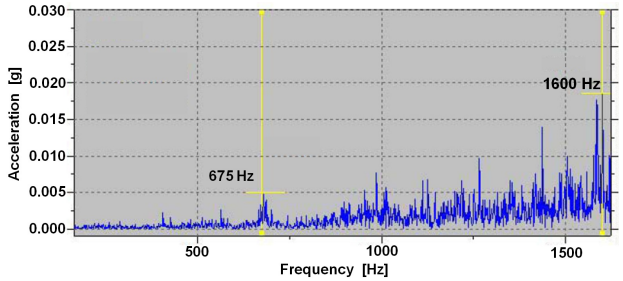

Fig. 17 Experimentally FFT spectrum; spindle turning at 1,000 *rpm*.

The methodology is based on the chip segmentation frequencies acquisition according to different cutting speeds and feed rates. The measurement of chip segmentation frequencies was realized by three methods:

- Acquisition, at a high frequency, of cutting forces and Labview FFT signal processing;
- Chip geometric measurement based on microscopic observations;
- FFT spectrum acquired using Vibroport 41 (Schenck) simultaneously with the signal for cutting forces in order to validate the segmentation frequency (figure 18). During this work, two working parameters were considered: the cutting speed Vc = 60-120 m/min and the feed rate f = 0.2-0.47 mm/rev. The cutting depth was kept equal to a constant value: ap = 1 mm.

In the following, it was proposed to study the frequency of the shearing plane formation. To do so, measurements at high-frequency sampling of cutting force signals were performed first. Then, geometrical measurements on the chip saw teeth were made. Finally, the frequency related to facet appearing on the machined surface was calculated and compared with the frequency acquired with Vibroport 41.

The aim of this section is to propose a calculation procedure dealing with the saw tooth frequency appearing during machining based on measurements on the chip section. Measurements are made using a microscope.

By considering the mean speed of chip evacuation on the tool rake face and the distance Δx_{chip} measured between two shearing planes the frequency can be established as:

$$F_{hzCG} = \frac{100 V_s}{6 \Delta x_{chip}}, \tag{5}$$

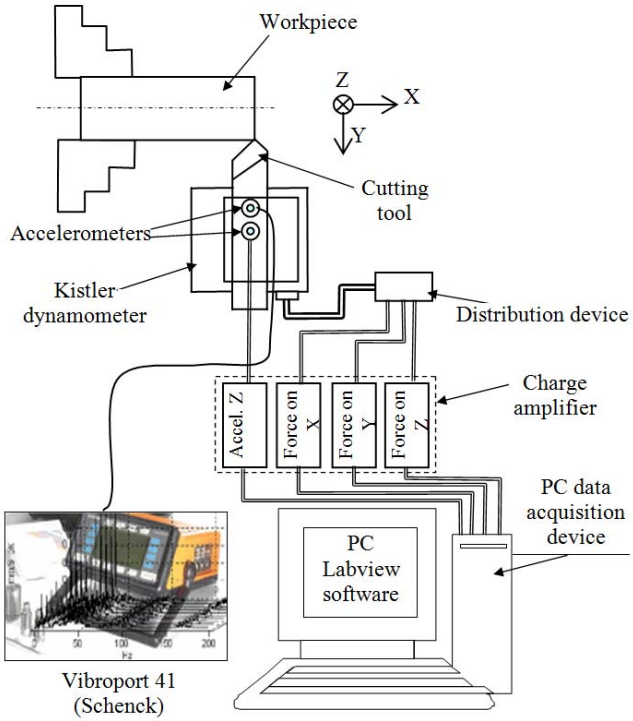

Fig. 18 Experimental acquisition chain in turning process

where F_{hzCG} is the frequency of the formation of shearing planes determined from chip geometry (Hz); V_s is chip slip speed on the tool rake face (m/min); Δx_{chip} is the distance between two consecutive shearing planes measured in the direction of the tool rake face (mm).

Assuming that the mass of the metal deformed during machining is constant, it can be written the following equation:

$$\rho_1 V_c f a_p = \rho_2 V_s e_c l_c. \tag{6}$$

ρ_1 and ρ_2 are the densities before and after deformation respectively (kg/cm^3); V_c is the cutting speed (m/min); f is the feed rate (mm/rev); a_p is the cut depth (mm); e_c is the chip thickness mean; l_c is the chip width (mm). Neglecting material compressibility, it is assumed that the ratio ρ_1/ρ_2 is equal to the unit. Consequently, the chip slip speed V_s on the tool rake face is given by the equation:

$$V_s = V_c \bullet \frac{f a_p}{e_c l_c}. \tag{7}$$

It appears that feed rate variation, for a fixed cutting speed, does not have a great influence on the appearance frequency of the shearing bands. This influence is larger when the cutting speed increases (figure 19 and 20). Frequency increases as the cutting speed increases; being a direct influence of the cutting speed on the chip evacuation speed -equation (7)

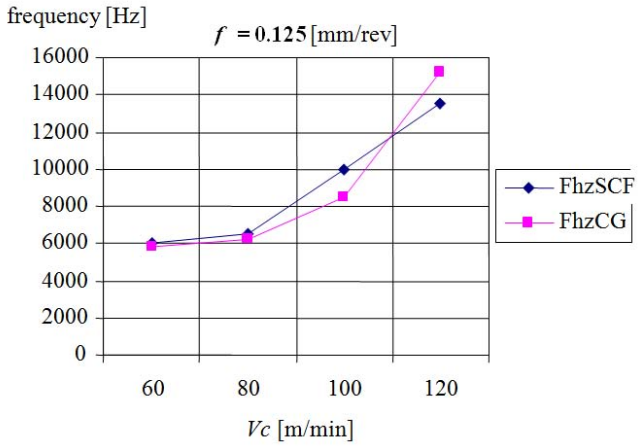

Fig. 19 Frequency accompanying saw-tooth chip formation depending on cutting speed f=0.2 (mm/rev)

Principal eigen frequencies values obtained with Vibroport 41 using module Transfer Function, for the assembly tool holder - Kistler dynamometer - support - transversal saddle are the followings: 150 Hz in Z direction, due to the assembly tool holder, in the case using four screws to fix the tool; 850 Hz in Y direction, 1,300 Hz in X direction and 2,400 Hz in Z direction, due by the assembly transversal saddle and Kistler dynamometer; eigen frequency in Z direction had a strong influence on the dynamical behaviour of the machine tool assembly.

Figure 21 presents an example of FFT spectrum acquired during hard turning. This is a good example of a

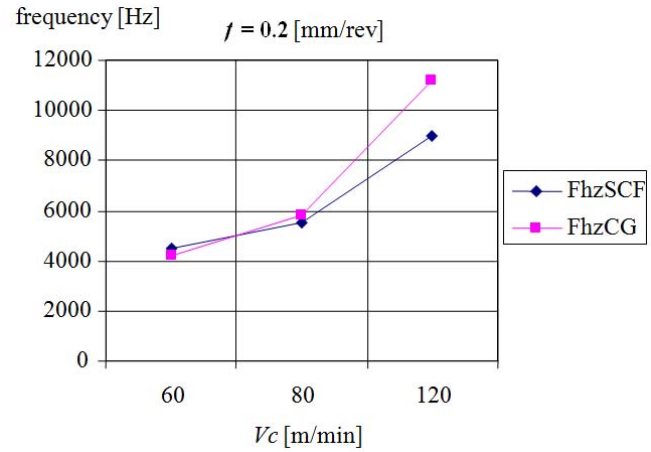

Fig. 20 Frequency accompanying saw-tooth chip formation depending on cutting speed f = 0.2 (mm/rev)

very easy separation of the chip segmentation frequency by the machine tool vibrations. Other two significant frequencies were 11,950 Hz and 17,925 Hz - the first two harmonics.

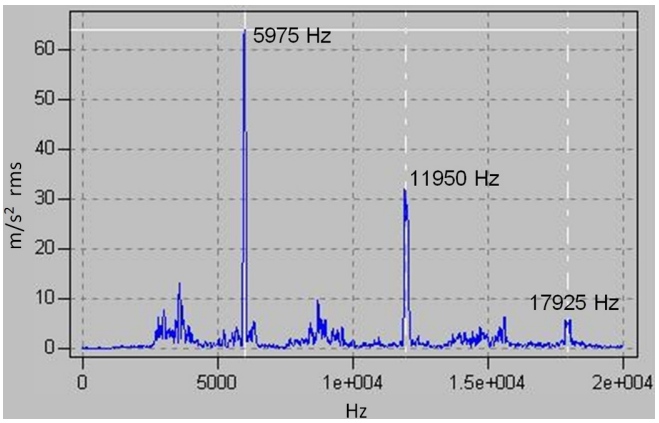

Fig. 21 Test with Vibroport 41; V_c=80 m/min; f=0.125 mm/rev

Figure 22 presents one significant example of a difficult case to separate the frequency of chip segmentation. The segmentation process appears at 6,087 Hz and the significant vibration of machine tool appears at 5,212 Hz. It was important to know and also avoid the frequency due to the instability signal. The useful domain considering the proper signal of transducers was 3 - 15,600 Hz. These limits are imposed by the piezoelectric accelerometers.

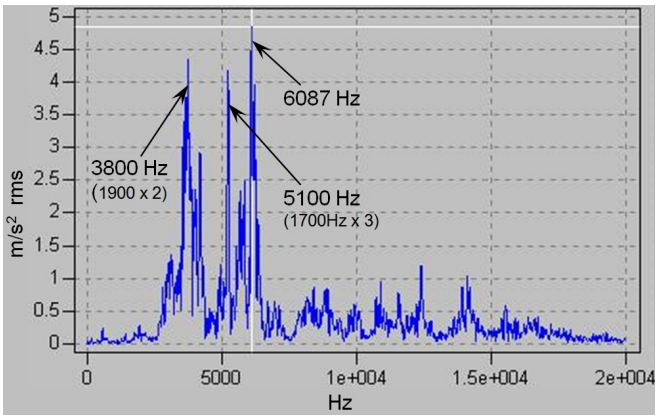

Fig. 22 Acquisition using V_c=60 m/min and f=0.05 mm/rev

4 Machine tool dynamic characterization - turning process recommendations

4.1 *An analysis according to three configurations*

The dynamic characterization of the machining system is supplemented by an analysis according to three configurations: electric motor drive, electric motor turning the spindle, electric motor turning the spindle and advance movement coupled [5]. The three axes accelerometer is placed on the tool body and the one-way accelerometer is located on the bed near the spindle. The frequencies values are presented in the figure 23 when the machine tool is not in charge with the cutting process, for the three configurations mentioned. The frequencies below 100 Hz, belong to the engine behaviour, the amplitudes are very weak, very low and appear on each tests configuration.

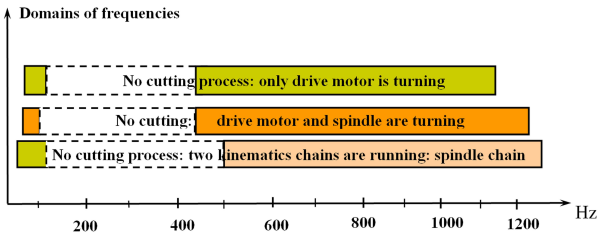

Fig. 23 Frequencies domains representation in the case with no cutting process.

The frequencies corresponding to no cutting process are given [6] for the three directions in the case of the kinematics chain "electric motor turning the spindle and advance movement coupled". The measured significant frequencies are into the domain of 230 Hz up to 1,000 Hz (see figure 24), and more, on the three x, y and z directions.

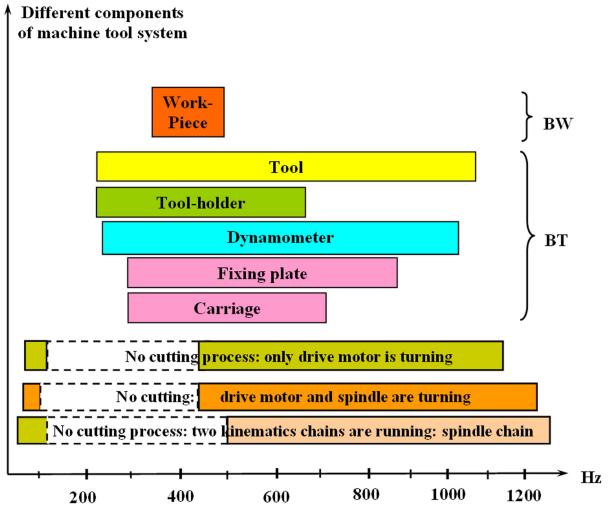

Fig. 24 Natural frequencies superposition in the case of no cutting process.

4.2 *About a better management of the cutting process*

In order to better manage the cutting process, the following recommendations are considered:

Increasing the workpiece rigidity. In order to reduce the vibrations problems at the time of the machining of the thin walls it is always well adapted, as known previously, to rigidify the part by an adapted fixture, when that is possible [30], [37], [31]. The process simulations allows us to specify before to have begun machining the most adapted solution, and even it is possible to redesign the shape of the workpiece in order to bring more rigidity to him.

Control of the cutting stiffness by reducing axial tool engagement. The theory of the stability lobes highlighted very early the importance of the relationship between the workpiece stiffness or the tool, and the cutting stiffness (the coefficient which links the tool displacement into the material to the cutting pressure, in the vibration direction). The most significant parameter to decrease this ratio is roughly speaking the projected cutting tool edge length in the material, which always impose to the specialists in machining process to naturally reduce the tool axial engagement [25], [34].

Modifying the cutting tool angles. Another way of decreasing the cutting stiffness is to exploit the tool angles so that the cutting pressure should be parallel with the wall. Thus the cutting stiffness would be theoretically null.

These two possibilities of stiffness control are major in the vibratory phenomenon during machining, in tools selection (angles, coatings etc.) and the strategies of machining in generally have the tendency to exploit these two effects [3], [28].

Limit the possibility to generate vibrations, avoid the resonance.

- Avoiding the frequencies with problems: by choosing the proper speed of the spindle (considering the stability lobes theory);
- Adding damping: by lubrication, controlling the pressure on the assembly surfaces, etc;
- Obtaining the excitation spectrum: by tools with variable step, by the spindle rotation with variable speed;
- Controlling actively: by the use of actuators (axes machine, turret etc.) controlled dynamically according to measurements, in order to eliminate the vibrations. For the moment, in practice, the achievements in this field are mainly regulations of average effort or power by the reduction of the tool advance [19], [2].

5 Conclusion

Within the framework of this study, the objective was to find (starting from the experimental tests in turning) a correlation between the frequency founded on the acquired FFT spectrum and the dynamic process based on the elastic system Machine tool, Workpiece and Tool device.

Machine tools and particularly, in this paper, the lathe, evolved to the limits of certain parameters of cutting that consist in a better control of the process. In this context, the subject "dynamic characterization" is very important and could help on the development of a simulation model for the cutting process on the machine tool.

This research was validated by experimental dynamic tests being based on measurements of the frequencies domain of the machining system Ernault HN400 lathe, in the LMP laboratory of the University of Bordeaux, France. Nevertheless, the method used is applicable to other machine tools also (milling, drilling etc.).

Taking into account the recommendations summarized in the section 4 the cutting process could be better managed.

The following step in our research will be to make a prediction for the cutting conditions and to supplement the necessary knowledge toward a global and industrial model of cutting process considering a 3D model in turning.

Acknowledgements

The authors acknowledge Jean Pierre Larivière CNRS (Centre National de la Recherche Scientifique - France) Engineer for the numerical simulation with SAMCEF® software. The authors would like also to thank the CNRS (UMR 5295) for the financial support to accomplish the project.

References

1. Albrecht, A., Park, S.S., Altintas, Y., Pritschow, G.: High frequency bandwidth cutting force measurement in milling using capacitance displacement sensors. Int. J. Mach. Tools Manuf. **45**, 993–1 008 (2005)
2. Bakkal, M., Shih, A.J., Scattergood, R.O.: Chip formation, cutting forces, and tool wear in turning of Zr-based bulk metallic glass. Int. J. Mach. Tools Manuf. **44**, 915–925 (2004)
3. Belhadi, S., Mabrouki, T., Rigal, J.F., Boulanouar, L.: Experimental and numerical study of chip formation during straight turning of hardened aisi 4340 steel. J. of Engng. Mech. **219**(B), 1–10 (2005)
4. Benardos, P.G., Mosialos, S., Vosniakos, G.C.: Prediction of workpiece elastic deflections under cutting forces in turning. Rob. and Computer-Integ. Manuf. **22**, 505–514 (2006)
5. Bisu, C.F., Darnis, P., Gérard, A., K'nevez, J.Y.: Displacements analysis of self-excited vibrations in turning. Int. J. Adv. Manuf. Technol. **44**(1–2), 1–16 (2009)
6. Bisu, C.F., Darnis, P., K'nevez, J.Y., Cahuc, O., Laheurte, R., Gérard, A., Ispas, C.: Nouvelle analyse des phénomènes vibratoires en tournage. Méc. & Indust. **8**, 497–503 (2007)
7. Bisu, C.F., K'nevez, J.Y., Darnis, P., Laheurte, R., Gérard, A.: New method to characterize a machining system: application in turning. Int. J. of Mat. Form. **2**(2), 93–105 (2009). Doi: 10.1007/s12289-009-0395-y
8. Cano, T., Chapelle, F., Lavest, J.M., Ray, P.: A new approach to identifying the elastic behaviour of a manufacturing machine. Int. J. Mach. Tools Manuf. **48**, 1 569–1 577 (2008)
9. Cardi, A.A., Firpi, H.A., Bement, M.T., Liang, S.Y.: Workpiece dynamic analysis and prediction during chatter of turning process. Mech. Syst. and Sign. Proces. **22**, 1 481–1 494 (2008)
10. Chandiranai, N.K., Pothala, T.: Dynamics of 2-dof regenerative chatter during turning. J. of sound vib. **290**, 448–464 (2006)
11. Chen, C.K., Tsao, Y.M.: A stability analysis of regenerative chatter in turning process without using tailstock. Int. J. Adv. Manuf. Technol. **29**(7–8), 648–654 (2006)
12. Chen, C.K., Tsao, Y.M.: A stability analysis of turning tailstock supported flexible work-piece. Int. J. Mach. Tools Manuf. **46**(1), 18–25 (2006)
13. Chiou, R.Y., Liang, S.Y.: Chatter stability of a slender cutting tool in turning with tool wear effect. Int. J. Mach. Tools Manuf. **38**, 315–327 (1998)
14. Chiou, Y.S., Chung, E.S., Liang, S.Y.: Analysis of tool wear effect on chatter stability in turning. Int. J. Mech. Sci. **37**(4), 391–404 (1995)
15. Couétard, Y.: Caractérisation et étalonnage des dynamomètres à six composantes pour torseur associé à un système de forces. Thèse de Doctorat, Université Bordeaux 1 (2000)
16. Dassanayake, A.V., Suh, C.S.: On nonlinear cutting response and tool chatter in turning operation. Communic. in Nonlin. Sci. and Num. Simul. **13**(5), 979–1 001 (2008)
17. Insperger, T., Barton, D.A.W., Stepan, G.: Criticality of Hopf bifucation in state-dependent delay model turning processes. Int. J. Non-Linear Mech. **43**, 140–149 (2008)
18. Iqbal, S.A., Mativenga, P.T., Sheikh, M.A.: A comparative study of the toolchip contact length in turning of two engineering alloys for a wide range of cutting speeds. Int. J. Adv. Manuf. Technol. **42**(1–2), 30–40 (2009)

19. Karabay, S.: Design criteria for electro-mechanical transducers and arrangement for measurement cutting forces acting on dynamometers. Mat. and Des. **28**, 496–506 (2007)
20. Karube, S., Hoshino, W., Soutome, T., Sato, K.: The non-linear phenomena in vibration cutting system. The establishment of dynamic model. Int. J. Non-Linear Mech. **37**, 541–564 (2002)
21. Koenigs, B.F., Tlusty, J.: Machine Tools Structures. Pergamon Press (1971)
22. Konig, W., Sepulveda, E., Lauer-Schmaltz, H.: Zweikomponenten schnittkraftmesser. Industrie-Anzeiger (1997)
23. Kudinov, V.A.: Dinamica Masinilor Unelten. Tehnicas, Bucarest (1970)
24. Lalwani, D.I., Mehta, N.K., Jain, P.K.: Experimental investigations of cutting parameters influence on cutting forces and surface roughness in finish hard turning of MND250 steel. J. Mat. Proc. Tech. **206**, 167–179 (2008)
25. Li, X.: Real-time prediction of workpiece errors for CNC for turning center, Part 4. Cutting-force-induced errors. Int. J. Adv. Manuf. Technol. **17**, 665–669 (2001)
26. Litak, G.: chaotic vibrations in a regenerative cutting process. Chao. Solit. and Fract. **13**, 1 513–1 535 (2002)
27. Litak, G., Kasperek, R., Zaleski, K.: Effect of high-frequency excitation in regenerative turning of metals and brittle materials. Chao. Solit. and Fract. **in press** (2007)
28. Mabrouki, T., Deshayes, L., Ivester, R., Rigal, J.F., Jurrens, K.: Material modeling and experimental study of serrated chip morphology. In: ENSAM-Cluny (ed.) 7^{th} CIRP International Workshop on the Modeling of Machining Operations, vol. 2. Cluny - France (2004)
29. Marinescu, I., Ispas, C., Boboc, D.: Handbook of Machine Tool Analysis. Deckker, M., New York (2002)
30. Mehdi, K., Rigal, J.F., Play, D.: Dynamic behavior of thin wall cylindrical workpiece during the turning process, Part 1: Cutting process simulation. J. Manuf. Sci. and Engng. **124**, 562–568 (2002)
31. Mehdi, K., Rigal, J.F., Play, D.: Dynamic behavior of thin wall cylindrical workpiece during the turning process, Part 2: Experimental approach and validation. J. Manuf. Sci. and Engng. **124**, 569–580 (2002)
32. Moon, F.C.: Dynamics and chaos in manufacturing process. Wiley, New York (1998)
33. Qi, K., He, Z., Li, Z., Zi, Y., Chen, X.: Vibration based operational modal analysis of rotor systems. Measurement **41**, 810–816 (2008)
34. Rao, B.C., Shin, Y.C.: A comprehensive dynamic cutting force model for chatter prediction in turning. Int. J. Mach. Tools Manuf. **39**(10), 1 631–1 654 (1999)
35. Rigal, J.F., Zapciu, M.: Etude du comportement dynamique du tour universel gallic 20. In: 11^{th} Int. Conf. Manuf. Syst. - ICMa'S -, vol. S6, pp. 195–199. 14-15 oct. Bucharest, Roumania (1998)
36. Risbood, K.A., Dixit, U.S., Sahasrabudhe, A.D.: Prediction of surface roughness and dimensional deviation by measuring cutting forces and vibrations in turning process. J. Mat. Proc. Tech. **132**, 203–214 (2003)
37. Sutter, G., Molinari, A.: Analysis of the cutting force components and friction in high speed machining. J. Manuf. Sci. and Engng. **127**, 245–250 (2005)
38. Tlusty, G.: Manufacturing processes and equipment. Prentice-Hall (2000)
39. Tobias, S.A.: Machine tool vibration. Blackie and Soon, London (1965)
40. Toh, C.K.: Static and dynamic cutting force analysis when high speed rough milling hardened steel. Mat. and Des. **25**, 41–50 (2004)
41. Tounsi, N., Otho, A.: Identification of machine-tool-workpiece system dynamics. Int. J. Mach. Tools Manuf. **40**, 1 367–1 384 (1999)
42. Wang, J., Gong, Y., Abba, G., Antoine, J.F., Shi, J.: Chip formation analysis in micromilling opeation. Int. J. Adv. Manuf. Technol. **45**(5–6), 430–447 (2009)
43. Yaldiz, S., nsacar, F., Saglam, H.: Comparaison of experimental results obtained by designed dynamometer to fuzzy model for predicting cutting forces in turning. Mat. and Des. **27**, 1 139–1 147 (2006)